RESEARCH ARTICLE

Editorial Process: Submission:12/23/2023 Acceptance:08/22/2024

Green Synthesis of Silver Nanoparticles Using *centratherum anthelminticum* Extract against Breast Cancer Cells

Javeed Hameed Husain[1], Deepan Arumugam[1], Mohamed Suhail Nawabjohn[1], Sekar Kumaran[2], Ashok Kumar Pandurangan[1]*

Abstract

Objective: According to an international survey, the cancer occurrence in the breast is the foremost in women. Surgery and chemotherapy remain the definitive treatment for the breast cancer. The bio-green methods of synthesizing silver nanoparticles are cost-effective and eco-friendly when parallel to physical and chemical methods. In addition, they effectively control pathogenic microorganisms. Former research studies reveal that kalijiri a common name for *Centratherum anthelminticum* is used as a traditional medicine for various ailments including anti-bacterial, anti-fungal, antidiabetic and anticancer. Our present research study focal points on the green synthesis of silver nanoparticles using aqueous seed extract of *Centratherum anthelminticum* and the evaluation of their antioxidant and cytotoxic activity. **Methods:** An aqueous extract of seeds from *Centratherum anthelminticum* was prepared by boiling it with distilled water. The silver nanoparticles were synthesized from the seeds of *Centratherum anthelminticum* and characterized by various methods such as UV-Visible spectroscopy, FT-IR, Transmission electron microscopy, DLS and X-ray diffraction to confirm the formation of nanoparticles. **Results:** The cytotoxic analysis of MDA-MB-231 cells was tested with the synthesized silver nanoparticles complex. The observed result was IC50 of 35.06±1.2 and it was not shown any toxicity to the non-cancerous cell line. **Conclusion:** In a nutshell, the synthesized silver nanoparticles from the seeds of *Centratherum anthelminticum* may be used for the treatment of breast cancer. Further studies are warranted to furnish the mechanism of action.

Keywords: Anticancer- MTT assay- MDA-MB-231 cells- kalijiri

Asian Pac J Cancer Prev, **25 (8)**, 2711-2721

Introduction

Breast cancer is the second most frequent cause of cancer death in women [1]. It was announced that breast cancer was the leading cancer among women in the year 2020 [2]. In Particular, two times the number of breast disease cases was recorded in women in the age group of 15 – 49 in emerging countries than in copious developed countries [3]. The reason for the difference in incidence was owing to factors such as geographic variation, lifestyle, socioeconomic status, racial/ethnic background, hereditary variations, ecological components, and nearness of known hazard factors. Moreover, the utilization of screening mammography, the stage of disease at diagnosis and the accessibility of proper care is also playing a part in elevating the breast cancer rate in women [4]. Different subtypes of breast cancers arise from different gene mutations occurring in a luminal or basal progenitor cell population, causing difficulty in BC diagnosis and treatment [5,6]. Based on the occurrence and the types and their stage the treatment approach will be either local or systematic which follows surgery, radiation therapy, chemotherapy and hormone and drug-targeted therapy. On occasion, the combination of drug medication actions can be tagged along to treat breast cancer. At present, in modern society nanoparticles can be used as a carrier to carry the drug into targeted cancerous cell lines [7,8]. Nanotechnology is referred to the term manufacture, portrayal, manipulation and application of structures by controlling shapes and sizes at the nanoscale level [9]. Nanotechnology is the most promising arena in present and also in future for generating new applications in biotechnology and biomedicine which are linked to nanomedicine [10]. The convergence between nanotechnology and nanomedicine has opened new roads in the pharmaceutical and therapeutic field [11,12]. Nanoparticles (NPs) are characterized that sizes between 1 and 100 nm. They show absolute novelty and enhanced properties taking into account their particular characteristics are size range from 1nm to 100nm, shape, and structure [13]. These compounds are becoming widespread for their use in medical

*[1]School of Life Sciences, B.S. Abdur Rahman Crescent Institute of Science and Technology, GST road, Vandalur, Chennai-600048, Tamil Nadu, India. [2]Department of Botany, Government Arts and Science College, Harur, Tamil Nadu, India. *For Correspondence: ashokkumar.sls@crescent.education*

applications and also for consumer products; with the potential for use as therapeutic compounds, transfection vectors, anti-microbial agents and fluorescent labels [14]. Nanoparticles can be categorized broadly as inorganic and organic NPs. Inorganic NPs incorporate semi-conductor, such NPs like ZnO, CdS ZnS and metallic NPs such as Au, Cu, Ag, and Aluminium and magnetic NPs like Fe, Co, and Ni while organic NPs incorporate carbon NPs like quantum dots, fullerenes and carbon nanotubes. Among different nanoparticles, Silver (Ag) possesses unique and good chemical, physical as well as biological properties [15,16]. Silver, in a colloidal form, is used for the treatment of bacterial infections in open wounds, and the preparation of ointments, bandages and wound dressings [17,18]. In addition, nanosilver is also known for its commercial application like contraceptive pills for women to prevent pregnancy and in agriculture and to free from disease it is used as a water disinfectant [19,20]. Silver Nanoparticles (AgNPs) have been used for antimicrobial, antifungal, antioxidant, and anti-inflammatory effects [21-24]. The nanoparticles can be synthesized using physical, chemical, and biological methods. The physical methods are initially used to give a low production [25]. The chemical method utilizes different chemical agents to reduce metallic ions to nanoparticles. This includes certain hindrances as there will be utilization of toxic chemicals and generation of hazardous by-products [26]. The organic molecules go through restrained assembly and make the molecules depend for the production of metal nanoparticles that has trustworthiness its benefit for the environment [27]. The major advantage of this biological technique is simplicity; less time-consuming, low toxicity, low cost, and high yield, and its biocompatibility add to its value [28]. Different natural resources have been used for the green synthesis of NPs: plants, plant products, bacteria, yeast, viruses, fungi and algae [29]. Among the organisms, plants appear to be the best applicants and they are reasonable for their large-scale biosynthesis of nanoparticles with different shapes and sizes [30]. Medicinal plants have been utilized for quite a long time to treat a variety of diseases and maintain health before the introduction of modern medicine [31,32]. Certain natural products have been applied for cancer chemoprevention to inhibit or repress carcinogenesis and to stifle the harm of malignancy. One of the therapeutic plants is *Centratherum anthelminticum* also named Kuntze, Kalajiri, and Somraj. The most common English name is black cumin or bitter cumin is a robust leafy plant that belongs to the Asteraceae family of flowering plants. This ethnomedicinal plant can be found in India, Himalaya Mountain, Khasi Mountain, Sri Lanka, and Afghanistan, and its bioactive compounds are widely used as a traditional herb against fever, cough and diarrhoea. Further studies have shown various pharmacological properties exhibited in the seeds of *C. anthelminticum*, such as anti-viral, anti-filarial, anti-microbial, anti-fungal and anti-diabetic activities [33-36]. Recently, we reported that, Vernodalin isolated from *Centratherum anthelminticum* shown to inhibit the proliferation of colorectal cancer cells [37]. We aimed to green synthesize and characterize the synthesized silver nanoparticles with *C. anthelminticum* seeds extract and study the cytotoxic potential against breast cancer cells.

Materials and Methods

Silver nitrate (AgNO3), Chloroform, Ammonia, Sulphuric acid, Ninhydrin and Ferric chorlirde were procured from SRL Chemicals, (India) and Dulbecco's modified Eagle's medium (DMEM) was procured from HiMedia, (India). All other chemicals were of analytical grade.

Aqueous seed extraction

C. anthelminticum seeds were purchased from the market by a local supplier. The aqueous seed extraction method was carried out in a ratio of 1:15. About two grams of *C. anthelminticum* seeds was weighed and taken in a conical flask. Then 30ml of distilled water was added to the conical flask. The conical flask was heated at 55 – 60° C in a water bath for 15 to 20 minutes. After the heating process, it was allowed to cool in a room temperature. Then the *C. anthelminticum* seed extract was filtered with Whatman No 1 filter paper and it was air dried. Further, the sample was stored for future use.

Phytochemical Analysis

C. anthelminticum aqueous seed extract was subjected to find the presence of the following phyto constituent's glycosides, quinones, saponins, amino acids, polyphenols, steroids and phytosterols.

Test for glycosides

2ml of *C. anthelminticum* seed extract was added to a test tube. To which 3ml of chloroform and 1ml of ammonia solution were added. The presence of glycosides in the extract was indicated by the pink colour.

Test for quinones

1 ml of seed extract was mixed with 1 ml of concentrated sulphuric acid in a test tube. The formation of red colour in a test tube confirms the presence of quinones.

Test for amino acids

Take 1 ml of seed extract in a test tube and add 1 ml of ninhydrin. The presence of amino acids was verified by the purple colour formation.

Test for saponins

1 ml of seed extract mixed with 2 ml of distilled water in a test tube. Then the test tube was shaken well, the formation of foam indicates the presence of saponins in the seed extract.

Test for polyphenols

2ml of *C. anthelminticum* seed extract in a test tube. Add 2 drops of ferric chloride and mix well. The formation of dark blackish-blue or green colour indicates the presence of polyphenols.

Test for steroids and phytosterols

2 ml of chloroform was taken in a test tube and mixed with 1 ml of aqueous seed extract along with a few drops

of concentrated sulphuric acid was added. Thus, results in the brown ring formation that indicates the presence of sterols and the bluish-brown ring be a sign of the phytosterols in attendance.

Synthesis of Silver Nanoparticle from C. anthelminticum seed extract

1ml of *C. anthelminticum* seed extract was diluted with 9ml of distilled water (1:9) and it was taken in two different test tubes and labelled as control (C) and test (T). To the test tube, 20µl solution of silver nitrate was added and kept for incubation at 37° C for 24 hrs. The colour change from yellow to dark brown indicates the formation of silver nanoparticles. The control sample without the addition of AgNO3 was used for further analysis [38].

Characterisation of Silver nanoparticles from C. anthelminticum seed extract

Stability of AgNPs

The *C. anthelminticum* seed extract synthesised AgNPs stability was recorded between 300nm and 700nm at different time intervals such as Day 3, Day 4, Day 5, Day 6 and Day 55. This was recorded by using Systronics Pl Based Double Beam Spectrophotometer 2202.

UV-Visible Spectroscopy

The formation of silver nanoparticles by the reduction of silver ions was determined by an Ultraviolet-Visible spectrophotometer instrument in the range of 200 to 800 nm. Distilled water was set as a control. This spectrophotometer analysis records the intensity of absorption (A) or optical density (O.D) as a function of wavelength. Absorbance is directly proportional to the path length, (L), and the concentration (c), of the absorbing species. To identify the presence of silver nanoparticles, the AgNPs were taken in a quartz cuvette and absorbance was measured in the 300 – 700nm wavelength range by using a UV-Vis spectrophotometer (Systronics Pl Based Double Beam Spectrophotometer 2202).

Fourier-Transform Infrared Spectroscopy

The FT-IR analysis of green synthesized silver nanoparticles was followed by NajeerAhamed et al. [39]. The FT-IR spectroscopy analyses the chemical composition or functional groups which are presented in the synthesized silver nanoparticles. They may be organic chemicals used in a whole range of applications or inorganic including polymers, drugs and adhesives etc. The isolation of organic compounds and characterization for any contamination can be done by Fourier Transform Infra-red Spectroscopy. The functional group of seed extract and silver nanoparticles was observed with a range of 500 cm-1 to 4000 cm-1 using FTIR (Jasco FT/IR-6300). The various modes of vibrations were recorded and types of functional groups present in the AgNPs were noted.

X-Ray Diffraction Study

The AgNPs powder was analysed by using XRD followed by the method Albura, [40]. The phase variety and grain size as well as the formation and quality of compounds of synthesized Silver nanoparticles are determined by X-ray diffraction spectroscopy. The dried powdered silver nanoparticles were coated on an XRD grid and their spectrum reading was noted at the voltage of 40kV and a current of 30mA with Cu K1 radiation of wavelength 1.5406 Å by using a Philips PW 1830 X-ray generator. The XRD pattern was scanned in the 2θ range from 30° to 70° with a step size of 0.04°/s.

Transmission Electron Microscopy

The size and morphology of silver nanoparticles were characterized by Transmission Electron Microscopy. In the TEM analysis, silver nanoparticles were prepared by coating an aqueous solution of silver nanoparticle drops on carbon-coated copper grids and made to dry for 5 min; the extra solution was discarded using blotting paper at room temperature.

Dynamic light scattering analysis

The changes in the diffusion behaviour of macromolecules from the solution can aid to determine the particle size in the suspension. A monochromatic beam of light (laser) is passed through the solution containing spherical particles in a Brownian motion causing a Doppler Effect which changes the wavelength of the incoming laser. The change relates to the size of the particle.

Antioxidant Activity

The 2,2-Diphenyl-1-picrylhydrazyl (DPPH) method was used to measure the antioxidant activity of AgNPs synthesized from *C. anthelminticum* aqueous seed extract by the method Satria et al., [41]. The different concentrations of 100, 200, 300, 400 and 500g/ml of *C. anthelminticum* seed extract and AgNPs were added with 4mM DPPH in methanol. This reaction mixture was shaken well and kept in incubation in a dark room for 30 minutes at room temperature. Later, the absorbance reading was recorded at 517nm. The lower absorbance of the reaction mixture indicates a high percentage of free radical scavenging activity. The percentage of free radical scavenging was determined by the following formula;

$$\%\text{inhibition} = (\text{control OD} - \text{sample OD}) / \text{control OD} \times 100$$

Cell culture

The MDA-MB-231 triple negative breast cancer and Vero cells were cultured in 25 cm2 culture flasks and incubated at room temperature 37°C in an atmosphere of 5% Carbon dioxide and 95% air. The cells were subjected to liquid growth media of DMEM with L-glutamine 2mM, sodium bicarbonate 1.5g/l, glucose 4.5g/l, HEPES (10 mM) and sodium pyruvate (1.0 mM) supplemented with 10% Fetal bovine serum (FBS), penicillin (100 U/ml) and streptomycin (100 µg/ml). The Cell confluence was measured using the trypan blue dye exclusion method. The Cells were sub-cultured when 85-90% confluence was obtained.

Cytotoxicity studies

The cell lines were obtained from National Centre for

Cell Sciences (NCCS). The cells were cultured in DMEM supplemented with 10% heat-inactivated Fetal Bovine Serum (FBS), 100 U/mL penicillin G and 100 µg/mL streptomycin (Hi-media) grown at 37 °C in a humidified atmosphere of 5% CO_2.

Subculture and Maintenance of cell line

The medium and Trypsin were thawed to room temperature. An inverted microscope can be utilized to examine the tissue culture bottles for the decay of cells, pH, opaque or cloudiness and growth. The cells were maintained until 85-90% confluent was obtained after it was used for the process of subculture. The medium was discarded in a discarding jar. The distance between the jar and the flask was maintained. 2ml of PBS was added and the flask was kept for 3 minutes. The PBS along with dead cells is discarded. Trypsin was added to the flask and incubated at 37 ºC for 3-5 minutes for disaggregation. Individual cells were observed and were present in a suspension. 5 ml of 10% DMEM with FBS was added using a serological pipette. The passage was done carefully by using a serological pipette. The process was repeated if any clumps were noticed. After passage through the cells, it was split into 1:2 and 1:3 ratios for Cytotoxicity studies.

Seeding of cells

After homogenization, the cell suspension was taken and poured into 96 well plates. In each well 1 x 10^6 cell suspension was added and kept in a 5% CO_2 atmosphere. After 2 days of incubation, observe the cells in an inverted microscope. The cells were grown until 90% confluence was observed.

Drug Testing

The 48hr monolayer culture of cancer cells was microscopically examined for confluent monolayer, turbidity and toxicity. The cells are maintained until 90% confluence was observed. The growth medium (DMEM) was removed using micropipette with a care. The monolayer of cells was washed twice with PBS to remove the dead cells and excess medium. To the washed cells, the drug at different concentrations such as 20, 40, 60, 80, and 100µg/mL was added and followed by the addition of 200 µL of medium (without FBS) to the respective wells of the 96 wells titer plates. To the control cells, 1ml DMEM without FBS was added (no drug). The plates were kept in incubation at 37 °C in a 5% CO_2 environment for 24 hrs and observed for cytotoxicity using an inverted microscope.

MTT assay

The Cytotoxicity effect of the drug was tested against the normal cell line (Vero) and the breast cancer cell line (MDA-MB 231) by MTT (3-(4,5-dimethylthiazol-2-yl)-2,5-diphenyltetrazolium bromide assay. MTT (3-(4,5-dimethylthiazol-2yl)-2,5-diphenyltetrazolium bromide is cleaved by mitochondria dehydrogenase in viable cells, yielding a measurable purple product formazan. Thus, the product formazan is an inverse variation to the level of cytotoxicity and direct proportion to the number of viable cells. After incubation, the medium was removed from the wells for MTT assay. Each well was washed with PBS. 20µg/ml of MTT (5mg/mL) was added. The plates were incubated for 3-4 hrs in a 5% CO_2 incubator. After incubation, the MTT was discarded and 200 µL of DMSO was added to each well and mixed gently and kept for 20 minutes. The Purple colour formation was observed. The wells were read at 595nm using 96 well plate readers (LISA microplate reader). The graph was plotted using the cell viability (%) at the Y-axis and the concentration of the sample on the X-axis. The formula used to calculate the cell viability percentage is as follows.

Cell Viability % = (O.D of the sample) / (O.D of cell control)*100

Results

Preparation of Aqueous seed extract of C. anthelminticum

In our current research study, the collected sample was dried, powdered and stored (Figure 1A). The aqueous extract was prepared by mixing powdered seed extract of *C. anthelminticum* along with distilled water and heating it in a water bath. The aqueous seed extraction of *C. anthelminticum* was noted to be yellow in colour.

Biosynthesis of silver nanoparticles from seed extract of C. anthelminticum

The colour conversion validates the reduction of silver ions to the silver nanoparticle. Silver Nitrate solution was colourless and it was mixed with an aqueous seed extract that is in yellow. After adding the AgNO3 solution, it starts to react and a change of colour from yellow to dark brown colour was observed due to the excitation of surface plasmon resonance leading to the formation of silver nanoparticles as shown in Figure 1B.

Phytochemical Analysis of C. anthelminticum

The Phytochemical constituents presented in the seed extract of *C. anthelminticum* were tabulated in Table 1. The colour change and results were shown in Figure 2A. From the tests, it was noted glycosides, quinones and amino acids are absent in the seed extract and the presence of saponins, polyphenol and steroids were observed.

DPPH Assay for Antioxidant Activity

The maximum inhibition of free radical scavenging activity was determined by the DPPH method and it was in the concentration of 500µg/ml for both the aqueous seed extract of *C. anthelminticum* and AgNPs. The

Table 1. Phytochemical Analysis of *C. anthelminticum*

S.No	Test Name	Result
1	Glycosides	Negative
2	Quinones	Negative
3	Amino Acid	Negative
4	Saponins	Positive
5	Polyphenol	Positive
6	Steroids	Positive

Figure 1. (A). The display of *Centratherum anthelminticum* (L.) Kuntze seeds. 2(B) Synthesis of AgNPs from the aqueous seed extract of *C. anthelminticum*. Colour change from yellow to dark brown indicating the synthesis of AgNPs.

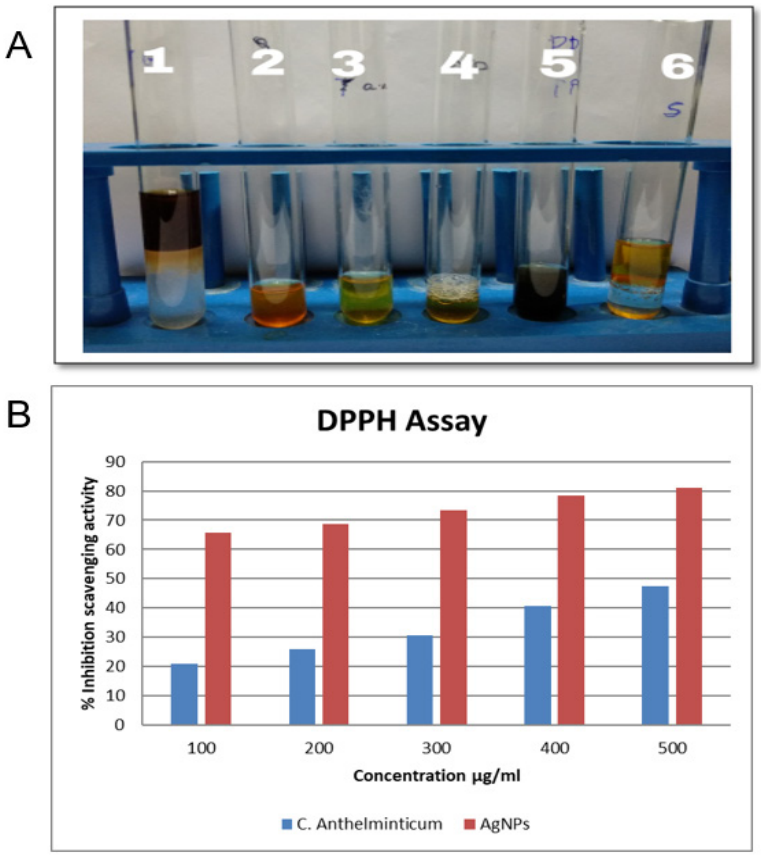

Figure 2. (A) Preliminary Phytochemical Analysis of *C. anthelminticum*. (B) Antioxidant Activity of *C. anthelminticum* seed extract by DPPH assay.

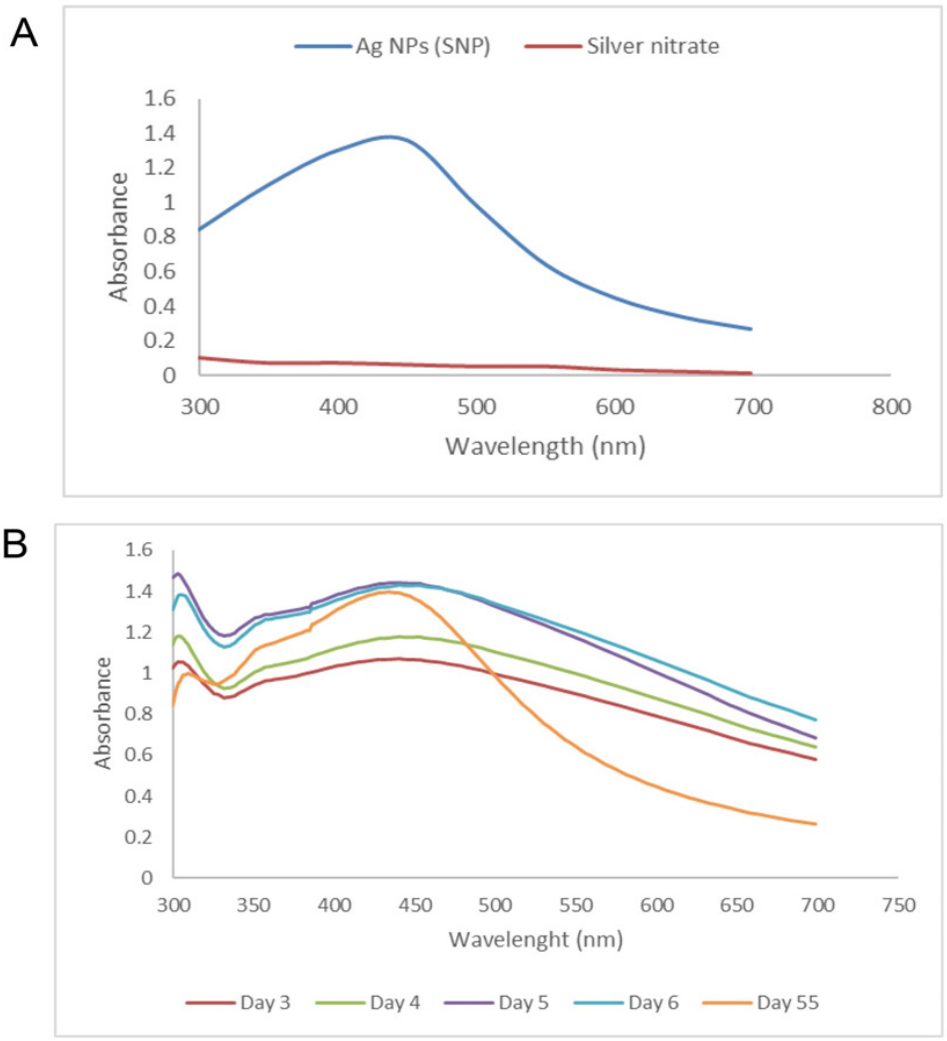

Figure 3. (A) UV - Visible Spectra for synthesised AgNPs and Silver nitrate. (B) UV spectrum of AgNPs was synthesized from *C. anthelminticum* extract at various time intervals.

concentration of an aqueous seed extract and synthesized silver nanoparticles tend to rise along with the free radicals as shown in Figure 2B.

Ultraviolet-Visible Spectroscopy

After the synthesis of silver nanoparticles, it undertakes different characterization methods. The reduction of pure Ag+ ions was monitored by using UV-Vis spectrophotometer after diluting a small aliquot of the sample into distilled water. The characteristic absorption peak at 428 nm in UV–Vis spectrum (Figure 3A) confirmed the formation of silver nanoparticles. The colourless AgNO3 do not show any reading on its own between 300nm to 700nm.

Stability of AgNPs

The stability of the reaction mixture was studied by using UV–Vis spectroscopy for several days. The UV–Vis spectrum was recorded for aqueous extract at different time intervals. The absorption peaks were marked in different coloured corresponding to the readings taken on aliquots removed for analysis at Day 3,4,5,6 and 55 respectively as shown in Figure 3B. The intensity of absorption and the peak wavelength of silver nanoparticles after 55 days remain constant. Thus, it was found that the colloidal mixture was stable for nearly 2 months, which was very supportive and convenient for the synthesis of nanoparticles. The surface Plasmon resonance (SPR) of silver nanoparticles produced a peak at the centre near 428nm, broadening of the peak indicated that the particles are polydispersed. The high constancy of green synthesized AgNPs of *C. anthelminticum* refers to there being no variation in the peaks even subsequent to a long incubation period of 2 months.

FTIR Analysis

The functional group of biomolecules was determined by FTIR analysis. The aqueous seed extract of *C. anthelminticum* shows the presence of nine bands at 3279.36, 2927.41, 1771.3, 1593.88, 1401.03, 1266.04, 1033.66, 811.885 and 513.936 cm–1 as represented in Figure 4A. The band at 3271 cm-1 is characteristic of the hydroxyl functional group in alcohol and phenol compounds and 2929.34 cm-1 is assigned to the aldehyde

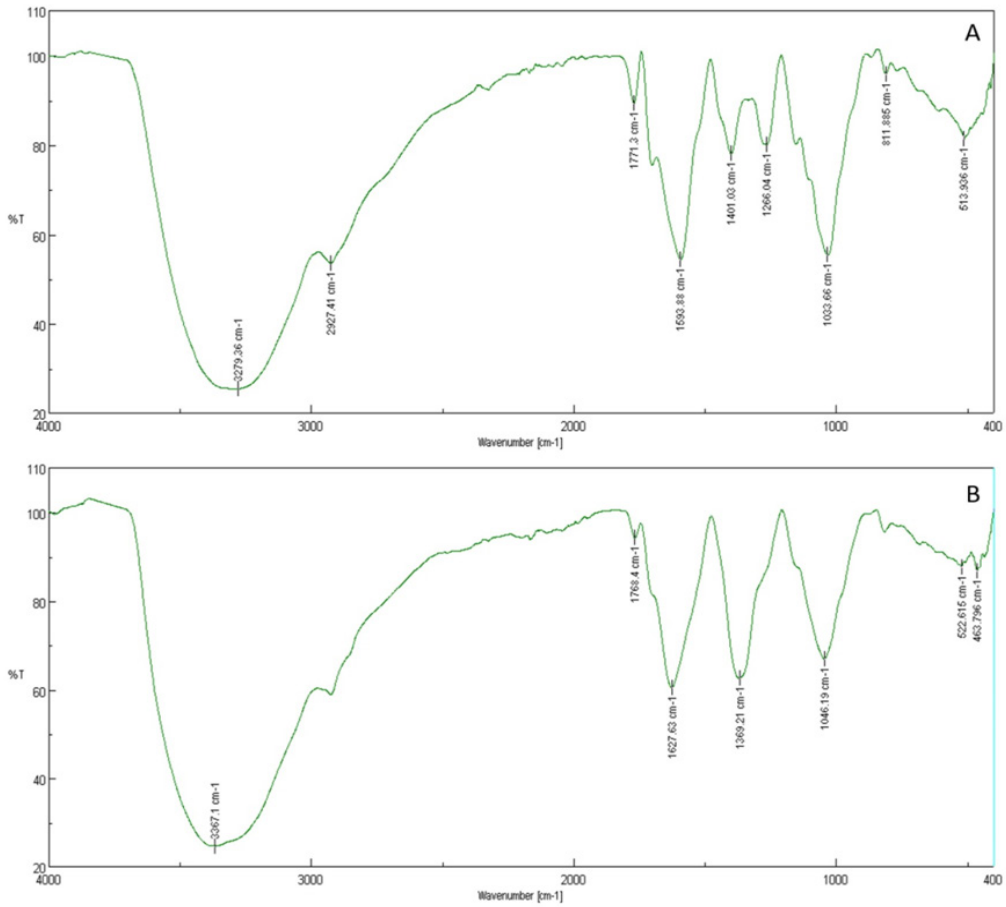

Figure 4. (A) Fourier transform infrared (FT-IR) spectrum of *C. anthelminticum* extract. (B) FT-IR spectrum of silver nanoparticles (AgNPs).

group, C-H stretching. The band seen at 1588.09 cm-1 is due to NH bending and 1397.17 cm-1 corresponds to the alkane group, CH3 bending. The band at 1044.26 cm-1 indicates C-O for the OH group. The bands at 819.598 cm-1 are assigned to the CH2 group out of plane deformation. The band at 774.279 cm-1 corresponds to C-H vibration and 610.36 cm-1 is due to C-Cl stretching. The band at 431.977 cm-1 corresponds to skeletal vibration. The AgNPs show the presence of seven bands at 3367.1, 1768.4, 1627.63, 1369.21, 1046.19, 522.615 and 463.796 cm–1 as represented in Figure 4B. The bands seen at 3280.32 cm−1 correspond to the OH-stretching vibrations of primary amines, respectively; while their corresponding bending vibrations were seen at 1641.13 cm−1 and 1556.27 cm−1 and 1392.35 cm−1 can be assigned to the C–N stretching vibrations of aromatic amines, the weak signal 1246.75 cm−1 corresponds to stretching signal of same C-N vibration of amine. The band at 1045 cm−1 corresponds to N-H deformation of amines respectively. The bands at 865.882 cm−1 and 611.324 cm−1 exemplify C-C Bending accordingly.

TEM Analysis

The morphology of AgNPs which are synthesized by *C. anthelminticum* shows a spherical shape. A sample of the synthesized silver nanoparticles is placed on a matrix that was copper coated with carbon particles and dried. Finally, images are pictured using TEM. The diameter of the nanoparticles is found to be 58nm. It is likewise discovered that the TEM picture indicates nanoparticles that are more or less uniform in size and shape as shown in Figure 5A.

DLS Analysis

The Dynamic Light Scattering size distribution image of biosynthesized silver nanoparticles is shown in Figure 5B. It was observed that the size distribution of AgNPs ranges from 30 to 60 nm. The average particle size distribution of AgNPs was calculated to be 58 nm.

XRD analysis

The synthesized AgNPs from the seed extract of *C. anthelminticum* were characterized by using XRD analysis. The diffraction intensity data are observed at 2θ from 10° to 70° and the diffraction pattern shown in Figure 5C corresponds to pure silver metal powder. Subsequent analysis of AgNPs precipitate by powder – XRD revealed some peaks at 40° (111), 46.1° (200), and 55.7° (311). The peaks revealed the formation of the silver is crystalline and its structure was face-centred cubic.

Cytotoxicity against Normal cell line and Breast Cancer cells (MDA- MB 213)

Figure 6A-B shows the cytotoxicity activity of

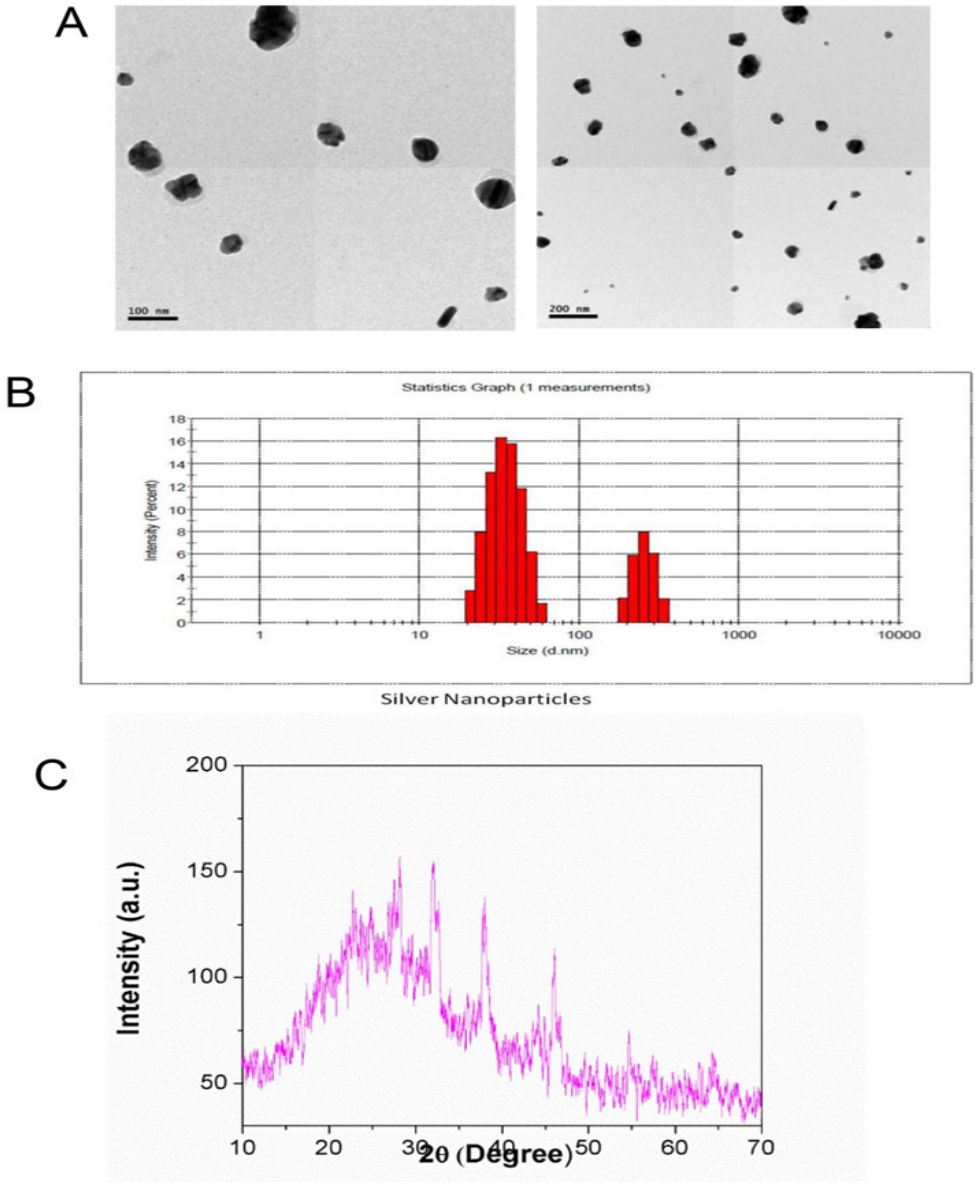

Figure 5. (A) TEM micrograph of the silver nanoparticles synthesized from C. anthelminticum. (B). DLS shows the mean average size of silver nanoparticles. (C). X-ray diffraction (XRD) pattern of silver nanoparticles (AgNPs) obtained by C. anthelminticum extract.

AgNPs from seed extract of selected plant against normal cell line by MTT (3-(4,5-dimethylthiazol-2-yl)-2,5-diphenyltetrazolium bromide assay. It was incorporated in 96-well microplates and incubated at 37°C for 24 h. The cells are mixed with the drug at different concentrations such as 10, 20, 30, 40, and 50µg/mL and incubated for 24 h. The cells are washed with buffer saline and MTT solution which was added to each well. The plates are allowed to stand at 37ºC in the dark area for 2 to 4 hours. The absorbance was read at 570 nm. The percentage of cell viability was calculated. After 24 hr, the alterations in the appearance of treated cells and control cells. The cytotoxicity activity of AgNPs from the seed extract of selected plant against breast cancer cell line by MTT assay was shown in Figure 6C. It is shown that upon increasing concentrations of silver nanoparticles solution, the deaths of cancer cells are also increased. When the cells were treated with the highest concentrations of silver nanoparticles (50µg/mL), they showed decreased cell viability (34%).

Discussion

Our current research study focuses on the green synthesis of silver nanoparticles using *C. anthelminticum* which has been done. *C. anthelminticum* is used extensively in traditional medicine to treat a range of diseases from skin disease vitiligo to hyperglycemia. It is considered to be anti-parasitic, antimicrobial and it is a good anti-oxidant. Since it has anti-microbial and anti-bacterial properties, the need of finding its anti-cancerous property is made in this research. The formation of silver nanoparticles is shown by the colour change from yellow to dark brown which indicates the reduction of the Ag+ ions. The colour change is due to the excitation of surface Plasmon vibrations [38]. In the Phytochemical analysis, it was investigated that saponins, polyphenols and steroids are present in *C. anthelminticum*, whereas

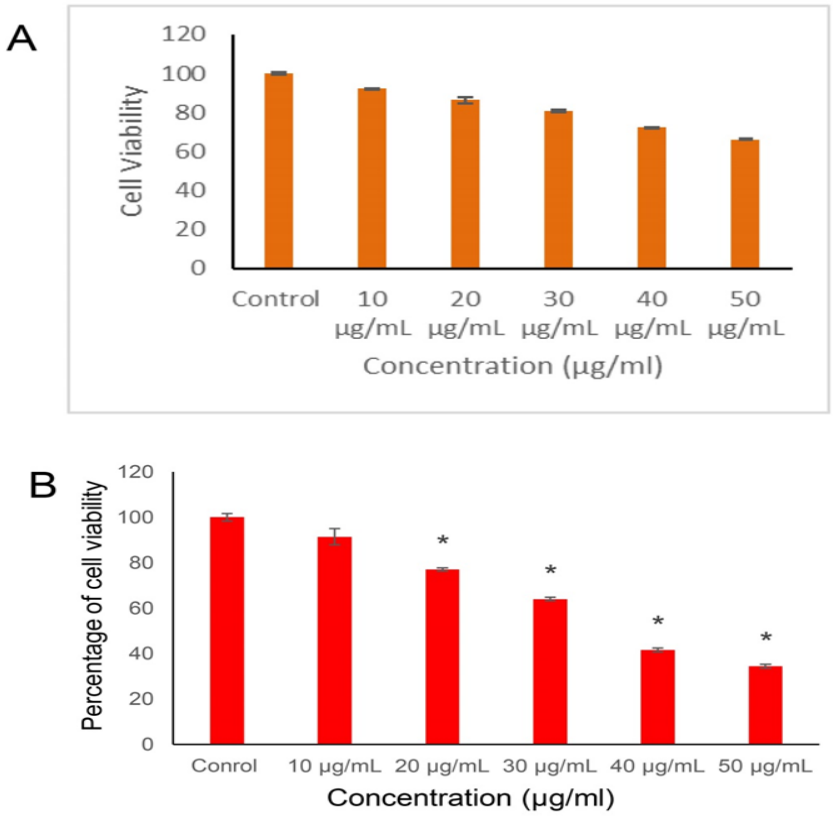

Figure 6. (A) In-vitro cytotoxicity of synthesized silver nanoparticle seeds of *C. anthelminticum* in Vero cell lines. Fig. (B) In-vitro cytotoxicity study of silver nanoparticle against MDA-MB 231 cell line. (C). Cytotoxicity of silver nanoparticle prepared by *C. anthelminticum* against Breast cancer cell line (MDA-MB 231): (A) control, untreated cell line, (B) 10µg/ml concentration treated cell line, (C) 20µg/ml concentration treated cell line, (D) 30µg/ml concentration treated cell line, (E) 40µg/ml concentration treated cell line, (F) 50µg/ml concentration treated cell line

Quinones, Glycosides and Amino Acid were found to be absent. Saponins induce apoptosis in tumour cells they are preferable drugs for the treatment of cancer because eliminating tumours cell by apoptosis is helpful to lower side effects in patients by avoiding necrosis [42]. Polyphenol is a good antioxidant and various studies have suggested that dietary polyphenols may protect against cardiovascular diseases, neurodegenerative diseases and some forms of cancer. Steroids are important biodynamic agents. The fascinating part in the development of drugs for diverse nuclear receptors is using polyphenols affinity in particular for the disorders which are conciliated by receptors. The Ultraviolet-Visible absorption spectrum of the reaction mixture was analysed at different wavelengths ranging from 350 to 700 nm. The characteristic absorption peak at 428 nm in UV–Visible spectrum confirmed the formation of AgNPs [43,23]. FT-IR analysis was carried out to identify the possible biomolecules responsible for the reduction of the silver ion and capping agent of bio-reduced silver nanoparticles by S. fusiformis. The shift in peak is attributed to the reduction of silver ions into nanoparticles. These records indicate the formation of silver ions due to a bio-reduction and their possible stabilization as nanoparticles. The TEM is the technique used to determine the size and size distribution of nanoparticle samples [44]. The TEM images revealed the formation of spherical and rounded rectangle-like structures. The size of the nanoparticle is around 10-60 nm. Similar results were observed by Murugesan et al. [45] using red alga Spyridia fusiformis. The XRD patterns obtained for the silver nanoparticles which are synthesized using *C. anthelminticum* extract some Bragg reflections with 2θ values of a set of peaks 40° (111), 46.1° (200), 55.7° (311). The peaks revealed the formation of the silver crystalline structure face-centred cubic. This was similar to the XRD results Mallmann et al. [46] in the green synthesis of silver nanoparticle [46,47]. According to a study of, Looi et al. [48] the in-vitro anti-proliferative effects of extracts from *C. anthelminticum* on human breast cancer were reported. Another study shows that chloroform fraction of *C. anthelminticum* (L.) seeds (CACF) inhibits the growth of MCF-7 human breast cancer cells. Chloroform fraction of CACF induces apoptosis by cell shrinkage, deformed cytoskeleton structure and DNA fragmentation [33]. Hence, the green synthesis of silver nanoparticles is toxic to human breast cancer cells and it has an incredible potential in biomedical applications.

In conclusion, green synthesis of silver nanoparticles using *Centratherum anthelminticum* extract has been reported. It is found that the extract we use is a good source for silver nanoparticle synthesis and is less time-consuming. The reaction is convenient and easy to handle. The quantity of extract is more important for determining the size distribution of silver Nanoparticle XRD and SEM studies have revealed the shape of the nanoparticles and the average size is 58 nm. The report states that the work

done has potential application for in vitro anticancer activity against human breast cancer cell line MDA-MB 231 and it also reveals some studies of anticancer drug discovery of *C. anthelminticum* synthesized silver nanoparticles.

Author Contribution Statement

All authors contributed equally in this study.

Acknowledgements

Conflict of interest

On behalf of all the co-authors, the corresponding author states that there is no conflict of interest.

References

1. Chan K, Morris GJ. Chemoprevention of breast cancer for women at high risk. Semin Oncol. 2006;33(6):642-6. https://doi.org/10.1053/j.seminoncol.2006.08.017.
2. Scudeler MM, Manóchio C, Braga Pinto AJ, Santos Cirino HD, da Silva CS, Rodrigues-Soares F. Breast cancer pharmacogenetics: A systematic review. Pharmacogenomics. 2023;24(2):107-22. https://doi.org/10.2217/pgs-2022-0144.
3. Forouzanfar MH, Foreman KJ, Delossantos AM, Lozano R, Lopez AD, Murray CJ, et al. Breast and cervical cancer in 187 countries between 1980 and 2010: A systematic analysis. Lancet. 2011;378(9801):1461-84. https://doi.org/10.1016/s0140-6736(11)61351-2.
4. Hortobagyi GN, de la Garza Salazar J, Pritchard K, Amadori D, Haidinger R, Hudis CA, et al. The global breast cancer burden: Variations in epidemiology and survival. Clin Breast Cancer. 2005;6(5):391-401. https://doi.org/10.3816/cbc.2005.n.043.
5. Hasanpourghadi M, Pandurangan AK, Mustafa MR. Modulation of oncogenic transcription factors by bioactive natural products in breast cancer. Pharmacol Res. 2018;128:376-88. https://doi.org/10.1016/j.phrs.2017.09.009.
6. Sims AH, Howell A, Howell SJ, Clarke RB. Origins of breast cancer subtypes and therapeutic implications. Nat Clin Pract Oncol. 2007;4(9):516-25. https://doi.org/10.1038/ncponc0908.
7. Hublikar LV, Ganachari SV, Patil VB, Nandi S, Honnad A. Anticancer potential of biologically synthesized silver nanoparticles using lantana camara leaf extract. Prog Biomater. 2023;12(2):155-69. https://doi.org/10.1007/s40204-023-00219-9.
8. Santhoshkumar M, Perumal D, Narenkumar J, Ramachandran V, Muthusamy K, Alfarhan A, et al. Potential use of bio functionalized nanoparticles to attenuate triple negative breast cancer (mda-mb-231 cells). Bioprocess Biosyst Eng. 2023;46(6):803-11. https://doi.org/10.1007/s00449-023-02858-5.
9. Ahmad B, Shireen F, Bashir S, Khan I, Azam S. Green synthesis, characterisation and biological evaluation of agnps using agave americana, mentha spicata and mangifera indica aqueous leaves extract. IET Nanobiotechnol. 2016;10(5):281-7. https://doi.org/10.1049/iet-nbt.2015.0053.
10. Chen X, Schluesener HJ. Nanosilver: A nanoproduct in medical application. Toxicol Lett. 2008;176(1):1-12. https://doi.org/10.1016/j.toxlet.2007.10.004.
11. Asharani PV, Hande MP, Valiyaveettil S. Anti-proliferative activity of silver nanoparticles. BMC Cell Biol. 2009;10:65. https://doi.org/10.1186/1471-2121-10-65.
12. Li J, Wang Q, Han Y, Jiang L, Lu S, Wang B, et al. Development and application of nanomaterials, nanotechnology and nanomedicine for treating hematological malignancies. J Hematol Oncol. 2023;16(1):65. https://doi.org/10.1186/s13045-023-01460-2.
13. Jahn W. Review: Chemical aspects of the use of gold clusters in structural biology. J Struct Biol. 1999;127(2):106-12. https://doi.org/10.1006/jsbi.1999.4123.
14. Su J, Zhang J, Liu L, Huang Y, Mason RP. Exploring feasibility of multicolored cdte quantum dots for in vitro and in vivo fluorescent imaging. J Nanosci Nanotechnol. 2008;8(3):1174-7.
15. Mousavi SM, Hashemi SA, Ghasemi Y, Atapour A, Amani AM, Savar Dashtaki A, et al. Green synthesis of silver nanoparticles toward bio and medical applications: Review study. Artif Cells Nanomed Biotechnol. 2018;46(sup3):S855-s72. https://doi.org/10.1080/21691401.2018.1517769.
16. Nieves LM, Mossburg K, Hsu JC, Maidment ADA, Cormode DP. Silver chalcogenide nanoparticles: A review of their biomedical applications. Nanoscale. 2021;13(46):19306-23. https://doi.org/10.1039/d0nr03872e.
17. Abbasi E, Milani M, Fekri Aval S, Kouhi M, Akbarzadeh A, Tayefi Nasrabadi H, et al. Silver nanoparticles: Synthesis methods, bio-applications and properties. Crit Rev Microbiol. 2016;42(2):173-80. https://doi.org/10.3109/1040841x.2014.912200.
18. Arora S, Jain J, Rajwade JM, Paknikar KM. Cellular responses induced by silver nanoparticles: In vitro studies. Toxicol Lett. 2008;179(2):93-100. https://doi.org/10.1016/j.toxlet.2008.04.009.
19. Hansen SF, Michelson ES, Kamper A, Borling P, Stuer-Lauridsen F, Baun A. Categorization framework to aid exposure assessment of nanomaterials in consumer products. Ecotoxicology. 2008;17(5):438-47. https://doi.org/10.1007/s10646-008-0210-4.
20. Madhumathi K, Sudheesh Kumar PT, Abhilash S, Sreeja V, Tamura H, Manzoor K, et al. Development of novel chitin/nanosilver composite scaffolds for wound dressing applications. J Mater Sci Mater Med. 2010;21(2):807-13. https://doi.org/10.1007/s10856-009-3877-z.
21. Hembram KC, Kumar R, Kandha L, Parhi PK, Kundu CN, Bindhani BK. Therapeutic prospective of plant-induced silver nanoparticles: Application as antimicrobial and anticancer agent. Artif Cells Nanomed Biotechnol. 2018;46(sup3):S38-s51. https://doi.org/10.1080/21691401.2018.1489262.
22. Mohsen LY, Fadhil Alsaffar M, Ahmed Lilo R, Khalil Al-Shamari A. Silver nanoparticles that synthesis by using trichophyton rubrum and evaluate antifungal activity. Arch Razi Inst. 2022;77(6):2145-9. https://doi.org/10.22092/ari.2022.358495.2235.
23. Nawabjohn MS, Sivaprakasam P, Anandasadagopan SK, Begum AA, Pandurangan AK. Green synthesis and characterisation of silver nanoparticles using cassia tora seed extract and investigation of antibacterial potential. Appl Biochem Biotechnol. 2022;194(1):464-78. https://doi.org/10.1007/s12010-021-03651-4.
24. Sampath G, Chen YY, Rameshkumar N, Krishnan M, Nagarajan K, Shyu DJH. Biologically synthesized silver nanoparticles and their diverse applications. Nanomaterials (Basel). 2022;12(18). https://doi.org/10.3390/nano12183126.
25. Ramasundaram S, Manikandan V, Vijayalakshmi P, Devanesan S, Salah MB, Ramesh Babu AC, et al. Synthesis and investigation on synergetic effect of activated carbon loaded silver nanoparticles with enhanced photocatalytic

and antibacterial activities. Environ Res. 2023;233:116431. https://doi.org/10.1016/j.envres.2023.116431.
26. Bar H, Bhui DK, Sahoo GP, Sarkar P, De SP, Misra A. Green synthesis of silver nanoparticles using latex of Jatropha curcas. Colloids and surfaces A: Physicochemical and engineering aspects. 2009;339(1-3):134-9.
27. Akay S, Yüksel G, Özad Düzgün A. Investigation of antibiofilm and antibacterial properties of green synthesized silver nanoparticles from aqueous extract of rumex sp. Appl Biochem Biotechnol. 2024;196(2):1089-103. https://doi.org/10.1007/s12010-023-04592-w.
28. Shah M, Fawcett D, Sharma S, Tripathy SK, Poinern GEJ. Green synthesis of metallic nanoparticles via biological entities. Materials (Basel). 2015;8(11):7278-308. https://doi.org/10.3390/ma8115377.
29. Makarov VV, Love AJ, Sinitsyna OV, Makarova SS, Yaminsky IV, Taliansky ME, et al. "Green" nanotechnologies: Synthesis of metal nanoparticles using plants. Acta Naturae. 2014;6(1):35-44.
30. Yu F, Takahashi T, Moriya J, Kawaura K, Yamakawa J, Kusaka K, et al. Traditional chinese medicine and kampo: A review from the distant past for the future. J Int Med Res. 2006;34(3):231-9. https://doi.org/10.1177/147323000603400301.
31. Kenchappa PG, Karthik Y, Vijendra PD, Hallur RLS, Khandagale AS, Pandurangan AK, et al. In vitro evaluation of the neuroprotective potential of olea dioica against aβ peptide-induced toxicity in human neuroblastoma sh-sy5y cells. Front Pharmacol. 2023;14:1139606. https://doi.org/10.3389/fphar.2023.1139606.
32. Khazaei S, Esa NM, Ramachandran V, Hamid RA, Pandurangan AK, Etemad A, et al. In vitro antiproliferative and apoptosis inducing effect of allium atroviolaceum bulb extract on breast, cervical, and liver cancer cells. Front Pharmacol. 2017;8:5. https://doi.org/10.3389/fphar.2017.00005.
33. Ananda Sadagopan SK, Mohebali N, Looi CY, Hasanpourghadi M, Pandurangan AK, Arya A, et al. Forkhead box transcription factor (foxo3a) mediates the cytotoxic effect of vernodalin in vitro and inhibits the breast tumor growth in vivo. J Exp Clin Cancer Res. 2015;34:147. https://doi.org/10.1186/s13046-015-0266-y.
34. Ashok P, Koti BC, Thippeswamy AH, Tikare VP, Dabadi P, Viswanathaswamy AH. Evaluation of antiinflammatory activity of centratherum anthelminticum (l) kuntze seed. Indian J Pharm Sci. 2010;72(6):697-703. https://doi.org/10.4103/0250-474x.84577.
35. Baig N, Sultan R, Qureshi SA. Antioxidant and anti-inflammatory activities of centratherum anthelminticum (l.) kuntze seed oil in diabetic nephropathy via modulation of nrf-2/ho-1 and nf-κb pathway. BMC Complement Med Ther. 2022;22(1):301. https://doi.org/10.1186/s12906-022-03776-x.
36. Singh O, Ali M, Husain SS. Phytochemical investigation and antifungal activity of the seeds of centratherum anthelminticum kuntze. Acta Pol Pharm. 2012;69(6):1183-7.
37. Mohebali N, Pandurangan AK, Mustafa MR, Anandasadagopan SK, Alagumuthu T. Vernodalin induces apoptosis through the activation of ros/jnk pathway in human colon cancer cells. J Biochem Mol Toxicol. 2020;34(12):e22587. https://doi.org/10.1002/jbt.22587.
38. Niraimathi KL, Sudha V, Lavanya R, Brindha P. Biosynthesis of silver nanoparticles using alternanthera sessilis (linn.) extract and their antimicrobial, antioxidant activities. Colloids Surf B Biointerfaces. 2013;102:288-91. https://doi.org/10.1016/j.colsurfb.2012.08.041.
39. NajeerAhamed MJ, Soundharajan R, Srinivasan H. Antibacterial, antibiofilm, and antivirulence effects of nanoparticles synthesized from colletotrichum gloeosporioides in pathogenic e.Coli. Microb Pathog. 2023;185:106420. https://doi.org/10.1016/j.micpath.2023.106420.
40. Alburae NA. Characterization and eco-friendly synthesis of silver and iron nanoparticles using microalgae extracts: Implications for nanobiotechnology. Pak J Biol Sci. 2024;27(4):210-8. https://doi.org/10.3923/pjbs.2024.210.218.
41. Satria D, Silalahi J, Haro G, Ilyas S, Hsb PA. Antioxidant and antiproliferative activities of an ethylacetate fraction of picria fel-terrae lour. Herbs. Asian Pac J Cancer Prev. 2017;18(2):399-403. https://doi.org/10.22034/apjcp.2017.18.2.399.
42. Henglein A. Physicochemical properties of small metal particles in solution: "Microelectrode" reactions, chemisorption, composite metal particles, and the atom-to-metal transition. J Phys Chem. 1993;97(21):5457-71. https://doi.org/10.1021/j100123a004.
43. Gopinath V, Velusamy P. Extracellular biosynthesis of silver nanoparticles using bacillus sp. Gp-23 and evaluation of their antifungal activity towards fusarium oxysporum. Spectrochim Acta A Mol Biomol Spectrosc. 2013;106:170-4. https://doi.org/10.1016/j.saa.2012.12.087.
44. Devi LS, Joshi SR. Ultrastructures of silver nanoparticles biosynthesized using endophytic fungi. J Microsc Ultrastruct. 2015;3(1):29-37. https://doi.org/10.1016/j.jmau.2014.10.004.
45. Subbiah M, Bhuvaneswari S, Vajiravelu S. Green synthesis, characterization of silver nanoparticles of a marine red alga spyridia fusiformis and their antibacterial activity. Int J Pharm Pharm Sci. 2017;9:192. https://doi.org/10.22159/ijpps.2017v9i5.17105.
46. Mallmann E, Cunha F, Agressott E, Menezes F, Barbosa R, Martins R, et al. Antifungal activity of nanobiocomposite films based on silver nanoparticles obtained through green synthesis. Curr Microbiol. 2023;80. https://doi.org/10.1007/s00284-023-03357-2.
47. Ferreyra Maillard APV, Bordón A, Cutro AC, Dalmasso PR, Hollmann A. Green one-step synthesis of silver nanoparticles obtained from schinus areira leaf extract: Characterization and antibacterial mechanism analysis. Appl Biochem Biotechnol. 2024;196(2):1104-21. https://doi.org/10.1007/s12010-023-04591-x.
48. Looi CY, Arya A, Cheah FK, Muharram B, Leong KH, Mohamad K, et al. Induction of apoptosis in human breast cancer cells via caspase pathway by vernodalin isolated from centratherum anthelminticum (l.) seeds. PLoS One. 2013;8(2):e56643. https://doi.org/10.1371/journal.pone.0056643.

This work is licensed under a Creative Commons Attribution-Non Commercial 4.0 International License.